COMBINED EFFECTS OF THE EFFECTIVE THERMAL CONDUCTIVITY AND ASH DEPOSIT THICKNESS ON THE RESULTS OF NUMERICAL SIMULATIONS

Nenad Dj. CRNOMARKOVIĆ [*1], Srđan V. BELOŠEVIĆ[1], Ivan D. TOMANOVIĆ[1], Aleksandar R. MILIĆEVIĆ[1], Andrijana D. STOJANOVIĆ[1], and Dragan R. TUCAKOVIĆ[2]

[1]Vinča Institute of Nuclear Sciences-National Institute of the Republic of Serbia, University of Belgrade, Mike Petrovića Alasa 12-14, Belgrade, Republic Serbia

[2]Faculty of Mechanical Engineering, University of Belgrade, Kraljice Marije 16, Belgrade, Republic Serbia

[*] Corresponding author; E-mail: ncrni@vin.bg.ac.rs

The most important thermophysical property for heat transfer through the ash deposits, accumulated at the waterwalls of the pulverized coal-fired furnaces, is the effective thermal conductivity. It affects the values of the wall variables: heat flux, temperature, and emissivity, and furnace temperature. In numerical simulations, the values of the effective thermal conductivity are used in combination with the ash deposit thicknesses. The objective of this investigation was to find the combined effects of the effective thermal conductivity and deposit thicknesses on the results of numerical simulations. Three curves were formed on the basis of the data available in literature. For every curve, three thicknesses of the non-uniform ash deposits were determined on the basis of the base normal distribution. The thickness of every surface zone was determined as a product of the number obtained from the diagram which shows dependence of the mean wall flux versus uniform thickness and corresponding thickness of the base distribution. The wall variables and flame temperatures were compared for the three values of the mean wall fluxes. The results showed that type of the curve did not influence the mean values of the wall variables and flame temperatures. The curves influenced the distribution of the wall variables very little. The maximal mean relative difference was obtained for the wall flux and it was less than 2%. The results indicates that the level of slagging can be defined by the ratio of the mean wall fluxes of the clean and wall covered by the ash deposit.

Key words: Numerical simulation, pulverized coal, furnace, waterwall, effective thermal conductivity, wall variables, ash deposit thickness, wall flux.

1. Introduction

During the combustion of pulverized coal inside a furnace, the coal mineral matter transforms into submicron and agglomerated ash particles of size 0.1-1 μm, and fly ash particles of size 1-20 μm. The ash particles are deposited on the furnace walls. The ash deposits are formed by several mechanisms: vapor and particle diffusion, thermophoretic and electrophoretic deposition, and inertial impaction [1]. Sarofim and Helble [2] estimated the deposition rates of the mechanisms (for one specific coal), and obtained $1.0*10^{-7}$, $4.0*10^{-7}$, and $1.8*10^{-4}$ g cm^{-2} s^{-1} for vapor condensation,

thermophoresis, and inertial impaction, respectively. The inertial impaction was the most important deposition mechanism for the pulverized coal ash deposition.

The ash deposits make the additional resistance to the heat transfer through the wall. It increases the temperature of the wall which in turn increases the loss of energy by radiation and reduces the heat absorbed from the flame. The emissivity of the deposits decreases with the increase in temperature and reduces the heat absorption. In this way, it also reduces the radiative loss by emission from the surface. The deposits are porous material, composed of the particles of various sizes and voids between them. As the heat transfer through the ash deposit consists of heat conduction and radiation, the transport property responsible for heat transfer is the effective thermal conductivity (ETC). Various values of the ETC can be found in literature. In numerical simulations, values of the ETC are connected with the ash deposit thicknesses. Bigger values of the ETC allows bigger thicknesses. This paper describes the combined effects of the adopted ETC of the ash deposits and ash deposit thickness on the results of numerical investigations.

The ETC of coal ash deposits and similar granular materials was investigated during the several past decades. Prasolov and Vainshenker [3] obtained ETCs for a number of coal ashes samples 0.046-0.256 W m^{-1} K^{-1} at temperature 333 K. Golovin [4] obtained ETCs for the anthracite ash samples the interval 0.012-0.023 W m^{-1} K^{-1}, at temperature interval 923-1173 K. Abryutin and Karasina [5] obtained the ETCs of Nazarovo subbituminous coal ash in the interval 0.093-0.140 W m^{-1} K^{-1} at 500 K and 0.128-0.174 W m^{-1} K^{-1} at 1000 K. Boow and Goard [6] measured the ETCs of ash deposits collected from the furnace walls, primary superheater, electrostatic dust, and one sample was laboratory ash, in temperature interval from 670 to above 1373 K. At the low temperature range, from 673 to 1173 K, the ETCs of each sample slowly increased with temperature. Their values were from 0.062 to 0.251 W m^{-1} K^{-1} (at 873 K). At the medium temperature interval, 1173-1373 K, an increase of ETC with temperature became steeper. At the high temperature interval, above 1373 K, the dependence of the ETC on temperature became steeper than at the medium temperature interval. At 1573 K, every sample was completely fused and the ETC of every sample was 1.88 W m^{-1} K^{-1}. Upon cooling, the ETC was bigger than that during the heating, because the physical condition of the ash sample was changed. It was found that the ETC increased with the increase in the particle size. Anderson et al. [7] obtained the same shape of the curve, but different boundaries of the temperature ranges. The temperature boundary of the medium interval was extended from 1273 to 1473 K, and the maximal temperature was 1723 K. The maximal value of the ETC was 2.8 W m^{-1} K^{-1} at 1723 K (heating cycle). The reason was found in different size of particles: in their experiment it was from 420 to 715 μm, while in the investigation of Boow and Goard [6] it was 200 μm. The values of the ETC in the low temperature interval were the same as those obtained by Boow and Goard. Rezaei et al. [8] measured the ETCs of four coal ash samples and two synthetic ash samples. They found an increase of the ETC with the increase in porosity and particle diameter. In comparison with the previous described results, they obtained bigger values of the ETCs. In the low temperature interval, from 573 to 873 K, the ETC was 0.5 W m^{-1} K^{-1}. The medium temperature interval was from 873 to 1073 K, and the maximal value of the ETC was about 1 W m^{-1} K^{-1}. Cundick et al. [9] defined the ETC for the particulate, sintered, and fused deposit layers for their study of heat transfer through the ash deposit layer. For the particulate deposit (low temperature interval, below 1000 K) it was 0.5 W m^{-1} K^{-1}, for the sintered deposit (medium temperature interval, from 1000 to 1600 K) it was 1.0 W m^{-1} K^{-1}, and for fused deposit (high temperature interval, above 1600 K) it was 5 W m^{-1} K^{-1}. Robinson et al. [10-13]

measured the ETC of samples obtained from co-firing of coal and wheat straw and samples of coal ash. For the 50-50% fuel blend, the ETC changed from 0.1 to 0.15 W m^{-1} K^{-1}, for the average deposit temperature of 748 K [10, 13]. For the pure coal combustion and for the same average deposit temperature, the ETC changed from 0.12 to 0.14 W m^{-1} K^{-1} [10, 13]. For the loose deposits of the fuel blends (65% coal, 35% wheat straw), the ETC was 0.14 W m^{-1} K^{-1} for average temperature interval of the deposit of 723 K [11, 12]. For the same sample and average temperature of 923 K (sintered deposit), the ETC was 0.31 W m^{-1} K^{-1} [11]. For the coal ash sample, the ETC was between 0.12 and 0.14 W m^{-1} K^{-1} for the low temperature interval. Richards et al. [14] numerically determined the deposit growth and its thermal properties from experimental data. They examined the deposit growth in the axisymmetric pilot scale reactor and found that ETC increased from 0.25 to 0.45 W m^{-1} K^{-1} as the surface deposit temperature increased from 600 to 1500 K. In addition, investigations revealed an increase of the ETC with the decrease in porosity [8, 15] and increase in particle diameter [6-8]. Coal ash composition is expressed in content of oxides of alkali and alkaline earth metals, with oxides of aluminum, silicon, iron, and titanium. Their thermal conductivities (of the compact material) are bigger than ETC of the ash samples and decrease with the increase in temperature from 300 to 1700 K [16]. Although the ETC increases with the increase in ash density and in content of iron oxides [6, 17], the chemical composition has small and indirect influence on the ETC [8, 15]. Some important and interesting aspects of the heat transfer through the porous bed can be found in [18, 19].

The average temperature of the sample represents its physical condition. In the low temperature range, deposit is in the particulate state and the ETC is in the interval 0.2-0.4 W m^{-1} K^{-1}. In the medium temperature range, the deposit is in the sintered state, while in the high temperature range the deposit is in the fused state. The diagram which shows the dependence of the ETC on temperature is a continuous curve. The highest value of the ETC is in the range 2-5 W m^{-1} K^{-1}. The values of the ETC directly affect the wall variables: wall flux, emissivity, and temperature. The bigger the values of the ETC, the smaller the wall temperature and bigger the wall flux for the same deposit thickness. The objective of this investigation was to find the difference of the results of a numerical investigation like wall variables and flame temperatures in the whole furnace and in the furnace exit plane, obtained for various combined values of the ETC and ash deposit thicknesses. The combined values should provide the same values of the mean wall fluxes, i. e. for the same level of the heat exchange in the furnace. The plan of the investigation was to compare the means of the wall variables and their distributions over the furnace walls for three curves which depict the dependence of the ETC on temperature. For the flame temperatures, means of the whole furnace and at the furnace exit plane would be determined. The first curve, curve A, is the one obtained by Boow and Goard [6] (the sample with the silica ratio 62). Its ETC was $K_{ef,A}$. For the second curve, curve B, it was $K_{ef,B} = K_{ef,A} + 0.1$ W m^{-1} K^{-1}, and for the third curve, curve C, it was $K_{ef,C} = K_{ef,A} + 0.2$ W m^{-1} K^{-1}. For example, at 873 K the ETC for the curve A is 0.251 W m^{-1} K^{-1}, for the curve B it is 0.351 W m^{-1} K^{-1}, and for the curve C it is 0.451 W m^{-1} K^{-1}. The investigation included the numerical simulations for uniform and non-uniform ash deposits. The investigation was expected to describe the importance of the selection of the ETC for the results of numerical investigations.

Figure 1 shows the values of the considered ETCs for curves A-C. In the low temperature range, when deposit is in the particulate state, the ETC of curve C is almost twice that of curve A. As the conductive heat transfer in nonmetallic solids is a consequence of the lattice vibrations and in gases by the molecule collisions [20, 21], and as the radiative emission is zero at 0 K, the ETC should be 0 W

m^{-1} K^{-1} at the temperature of 0 K. Strictly, that condition is satisfied only for curve A. For curves B and C, we can assume that approximations of the ETCs are acceptable in the considered temperature interval.

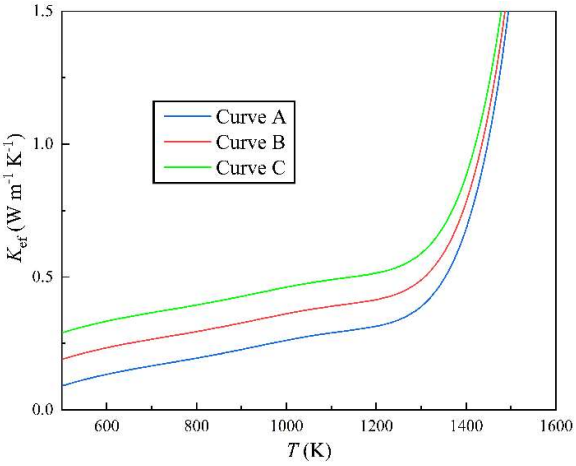

Figure 1. The effective thermal conductivities

The furnace of 210 MW monobloc thermal unit was selected (A2 TENT, located in Obrenovac, Serbia) in the investigation. The furnace is tangentially fired by Kolubara lignite and equipped with six jet burners (four tiers each), five of which are in operation. The furnace is 40 m high, 15.5 m wide, and 13.5 m deep. In the following text, mathematical model of the process inside the furnace, results and conclusions are described.

2. Mathematical model and method of the analysis

Mathematical model of the process inside the furnace described turbulent two-phase chemically reactive flow with radiative heat exchange. The model based on the time-averaged physical quantities was described [22]. The main features are briefly mentioned here. The gas phase is described by the time-averaged differential equations in the Eulerian reference frame, whereas the dispersed phase is described by the differential equations of the motion and change of mass and energy in Lagrangian reference frame. Heterogeneous reactions of coal combustion are modeled in the kinetic-diffusion regime. The zonal model of thermal radiation was applied through the CCTEA method [23]. The system of equations was closed by the k-ε model of turbulence. The thermophysical properties of the gas-phase were determined from the equation of state, tabulated values, and empirical relations. The system of equation was solved by the finite-difference method, while the discretization and linearization of the gas-phase equations were achieved by the control volume method and hybrid differencing scheme. Stability of the iterative calculation was provided by the under-relaxation method.

The ETC of the ash deposit was described by the equation:

$$K_{\mathrm{ef},i}(T) = \sum_{i=1}^{7} a_j \left(\frac{T}{1000}\right)^j + a_{0,i} \tag{1}$$

where the coefficient $a_{0,i}$ equals 0 (curve A), 0.1 (curve B), and 0.2 W m^{-1} K^{-1} (curve C). The coefficients a_j were given in [24]. As the only difference in the mathematical model is the value of the coefficient $a_{0,i}$, the investigation actually shows the impact of that coefficient on the results of numerical investigation.

Figure 2 shows impact of the ETC and deposit thickness on the radiative heat exchange between the flame and waterwalls. For the same thickness, the smallest heat exchange is obtained for curve A, then for curves B and C. Similarly, for the same heat exchange, the smallest deposit thickness is for curve A, followed by curves B and C. Curve B is approximately in the middle between curves A and C, so that the position of any curve between them (or for the coefficient $0 \le a_{0,i} \le 0.2$) can be assumed. For the infinite ETC, the corresponding curve in Fig. 2 would be a horizontal line.

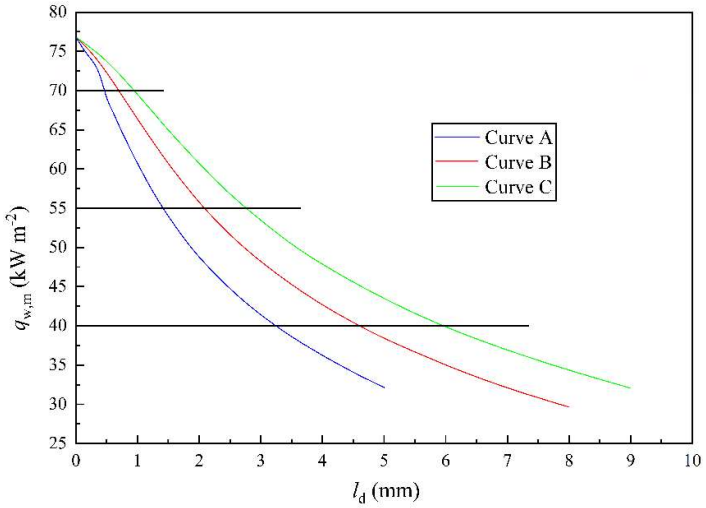

Figure 2. The mean wall flux for uniform deposit thicknesses

Three values of $q_{w,m}$ were selected: 40, 55, and 70 kW m^{-2}, and for each curve in the diagram, the thicknesses of the uniform ash deposit were found from the intersection of the horizontal lines with the corresponding curves. The parameters of the normal distributions of the ash deposit thicknesses were given in Tab. 1 which also shows the designation of the variables. For example, the string A55 means that the result was obtained for the normal distribution $N(1.412;0.424)$.

Table 1. The parameters of the normal distributions of the ash deposit thickness in (mm), $\mu;\sigma$

	$q_{w,m}$ (kW m^{-2})		
Curve	40	55	70
A	3.234;0.973	1.412;0.424	0.463;0.139
B	4.588;1.376	2.093;0.628	0.697;0.209
C	5.938;1.781	2.765;0.830	0.942;0.283

The non-uniform ash deposits were formed as normal distributions, as it was described that the radiative heat exchange for the normal distribution was close to that of the uniform thickness, when the mean value of the distribution is equal to the thickness of the uniform ash deposit [25]. Figure 2

shows the mean wall fluxes obtained for the selected ETCs for the uniform ash deposit thicknesses. That thicknesses are actually the values of the means of the normal distributions. The thicknesses of the normal distributions were obtained as a product of the thicknesses obtained as the intersection of the wall flux curves with horizontal lines with the corresponding thickness of the base distribution $N(1.0;0.30)$, as shown in Fig. 2. In that way the normal distributions were formed, with $\mu = l_d\mu_b$ and $\sigma = l_d\sigma_b$, where $\mu_b = 1$ and $\sigma_b = 0.3$ are the mean and standard deviation of the base distribution, respectively. The variation coefficient, defined as the ratio σ/μ, was kept constant for all distributions. The base distribution was formed by the subroutines given in [26].

Mean values of the wall variables were determined by formula (2):

$$\eta_m = \frac{\sum_i \eta_i}{N_{sw}} \tag{2}$$

where Nsw designates the total number of surface zones that are solid wall and η designate the variable. The mean flame temperatures were also determined by formula (2), with the exception that the total number of surface zones was replaced by the total number of control volumes Ncv. The mean temperatures in the furnace exit plane were determined in the same way, taking into account that Ncv designates the total number of control volumes in the furnace exit plane.

The relative difference in the distribution of the wall variables over the furnace walls were determined by formula (3):

$$\delta_{\eta,cr,mf,i} = \frac{\left|\eta_{cr,mf,i} - \eta_{A,mf,i}\right|}{\eta_{A,mf,i}} * 100 \tag{3}$$

where cr stands for curves B or C and mf stands for the mean flux. The means of the relative differences were obtained by formula (2).

3. Results and discussion

The mean flame temperature $T_{f,m}$ in the whole furnace and mean flame temperature in the furnace exit plane $T_{fe,m}$ are given in Tab. 2. For the mean wall fluxes of 40 and 55 kW m^{-2}, the mean temperatures in the furnace exit plane are bigger than mean temperatures in the furnace, whereas for 70 kW m^{-2} they are almost the same. The increase of the temperature in the furnace exit plane is obtained for an increase in the ash deposit thickness. For the same absorbed flux, the increase in deposit thickness increases the wall temperature, which then in turn increases emission from the surface and decreases the (net) wall flux. The flame temperature and relative differences for curve A were shown in Fig. 3a-c. The flame temperature is the highest at the area of intensive combustion, in the vicinity of burners. The furnace aerodynamics and radiation keep the high-temperature area far from the furnace walls. The temperature drops toward the furnace exit because of the radiative heat exchange with waterwalls. The relative differences are small, and the biggest values are obtained in the hopper bottom and in the vicinity of burners.

Table 2. The flame temperature means $T_{f,m}$ (K) (left) in the whole furnace and the flame temperature means in the furnace exit plane temperature $T_{fe,m}$ (K) (right)

	$q_{w,m}$ (kW m^{-2})			$q_{w,m}$ (kW m^{-2})		
Curve	40	55	70	40	55	70
A	1413.3	1362.0	1316.3	1459.1	1386.6	1314.9
B	1411.2	1361.3	1315.1	1458.1	1386.6	1313.4
C	1410.2	1360.8	1315.1	1458.1	1386.4	1313.2

The results given in Tab. 2 show that for each curve of the ETC and the same value of the exchanged heat similar mean flame temperatures were obtained, which is in accordance with the heat balance. For the mean wall flux of 70 kW m^{-2}, the mean temperature in the furnace outlet are the same as the mean temperatures in the furnace. As the mean wall flux decrease, both mean flame temperatures increase, with the difference that the mean flame temperature in the furnace exit is bigger than the mean temperature in the furnace. That is a consequence of the increased radiation from the walls, which are hotter and hotter for the increase in the wall thickness.

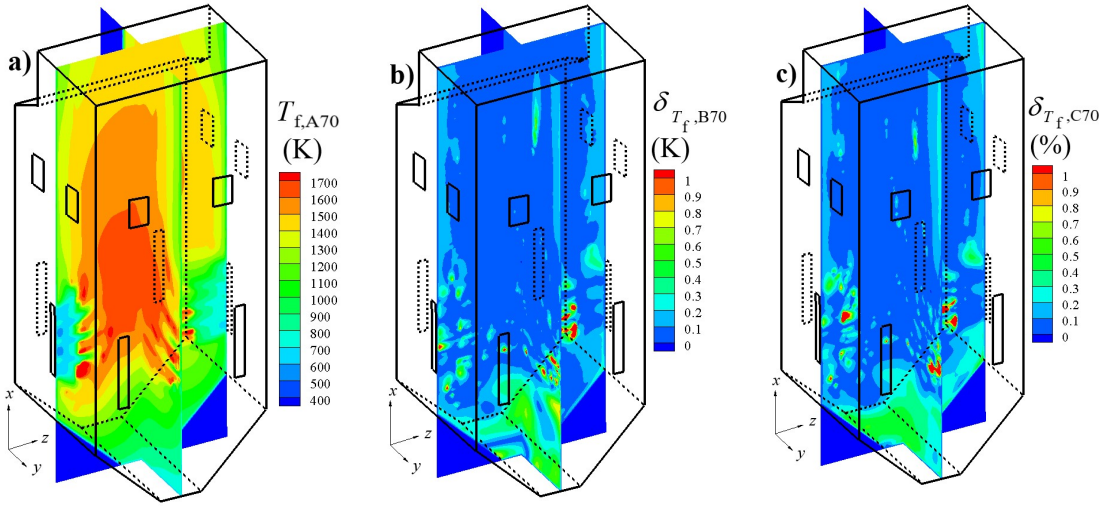

Figure 3. The flame temperature: (a) the value for $T_{f,A70}$; (b) the relative difference $\delta_{T_f,B70}$; (c) the relative difference $\delta_{T_f,C70}$

The mean values of the wall emissivities and wall temperatures are given in Tab. 3. From these results, it is evident that each curve of the ETC produces similar mean values of the wall variables for the same value of the mean wall flux. As already obtained, mean wall emissivity decrease and mean wall temperature increase with the increase in the ash deposit thickness.

Table 3. The mean wall emissivities ϵ_w (-) (left) and wall temperatures T_w (K) (right)

	$q_{w,m}$ (kW m^{-2})			$q_{w,m}$ (kW m^{-2})		
Curve	40	55	70	40	55	70
A	0.642	0.706	0.797	1175.9	1005.2	813.9
B	0.645	0.707	0.799	1171.9	1003.1	807.8
C	0.647	0.708	0.700	1169.7	1001.5	806.5

The means of the relative differences of the wall variables are given in Tab. 4. It is obvious that the relative differences increase when curve A is replaced by curves B or C, or it can be said that the relative difference increase with the increase in the value of the coefficient $a_{0,i}$. The relative differences are small, and the maximal mean relative difference obtained for the wall flux is less than 2%.

Table 4. The mean relative differences δ_m (%) of the wall emissivity (left), wall temperature (middle), and wall flux (right)

	$q_{w,m}$ (kW m^{-2})			$q_{w,m}$ (kW m^{-2})			$q_{w,m}$ (kW m^{-2})		
Curve	40	55	70	40	55	70	40	55	70
B	0.426	0.268	0.228	0.470	0.446	0.773	1.202	0.860	0.456
C	0.676	0.416	0.273	0.737	0.696	0.959	1.829	1.288	0.628

The distribution and relative differences of the wall fluxes, emissivities and temperatures over the front wall are given in Figs. 4-6. The biggest values of the wall fluxes and temperatures are obtained in the vicinity of burners, as expected, because of the vicinity of highest flame temperatures and intense emission of radiative energy. At the same area, the wall emissivities are the smallest, because of their dependence on temperature. For the same reason, the wall temperatures are the highest at that area. Although the considerable decrease of the wall flux from 70 to 40 kW m^{-2}, the ash deposit remains in the particulate state. Small differences of the wall fluxes obtained for each value of the total exchanged heat are clear. It is evident that the relative differences for curve B are smaller than for curve C, for all wall variables.

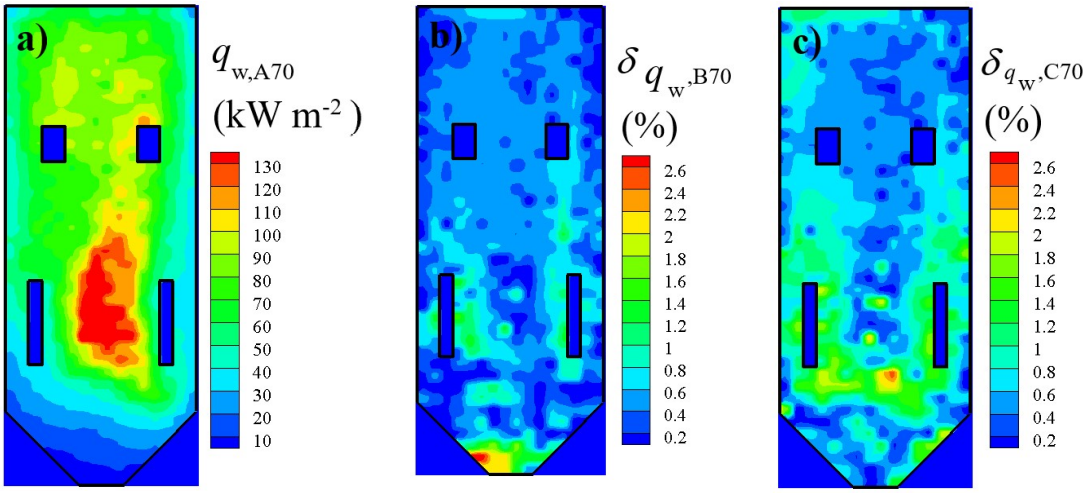

Figure 4. The wall flux, front wall: (a) the value for $q_{w,A70}$ (kW m^{-2}); (b) the relative difference $\delta_{q_w,B70}$; (c) the relative difference $\delta_{q_w,C70}$

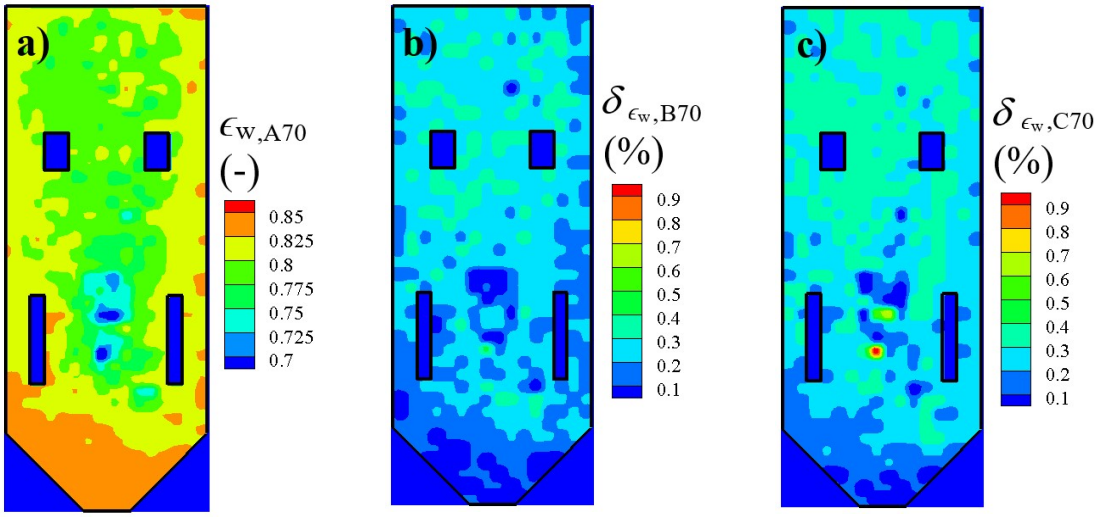

Figure 5. The wall emissivity, front wall: (a) the value for $\epsilon_{w,A70}$ (-); (b), the relative difference $\delta_{\epsilon_w,B70}$; (c) the relative difference $\delta_{\epsilon_w,C70}$

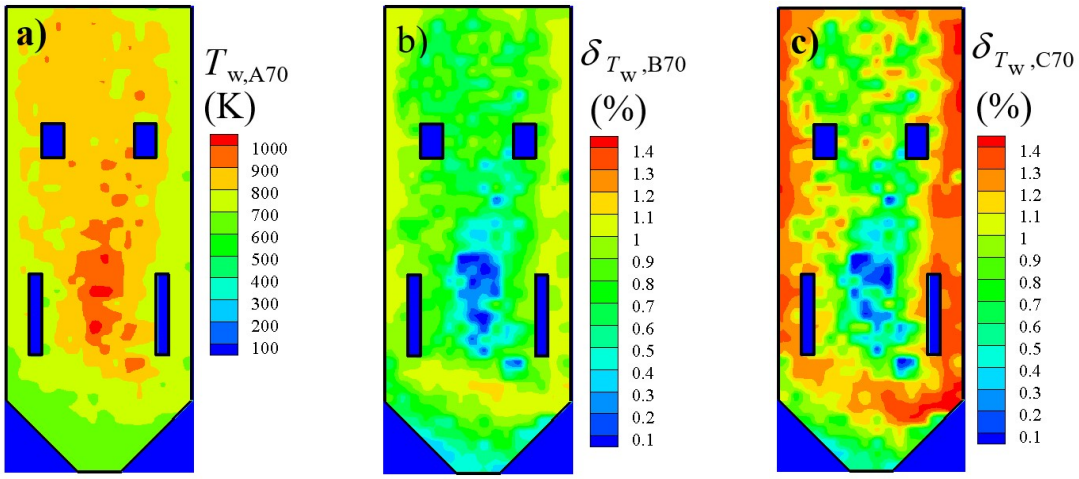

Figure 6. The wall temperature, front wall: (a) the value for $T_{w,A70}$, (K); (b) the relative difference $\delta_{T_w,B70}$,; (c) the relative difference $\delta_{T_w,C70}$

The thicknesses of the uniform deposits are actually means of the normal distributions given in Tab. 1. The relative differences of the wall variables are given in Tab. 5. As for the non-uniform deposits, the relative differences are small. The maximal mean relative difference is less than 2%. The relation between the means of the flame temperatures and wall variables are expected to be the same as for the non-uniform ash deposits.

Table 5. The mean relative differences δ_m (%) of the wall emissivity (left), wall temperature (middle), and wall flux (right), for the uniform deposits

	$q_{w,m}$ (kW m^{-2})			$q_{w,m}$ (kW m^{-2})			$q_{w,m}$ (kW m^{-2})		
Curve	40	55	70	40	55	70	40	55	70
B	0.427	0.269	0.240	0.423	0.431	0.788	1.147	0.778	0.456
C	0.683	0.406	0.290	0.664	0.662	0.975	1.756	1.181	0.619

The investigation shows that for the uniform thickness of the ash deposit, the level of slagging is defined by the ratio $q_{w,m}/q_{w,m0}$, where $q_{w,m0}$ = 76.82 kW m^{-2} is the mean wall flux for the clean wall, as previously assumed [27]. Whenever that ratio is the same, the results of numerical simulation of the investigated furnace are similar, for the uniform deposits. When the objective of the investigation is to find the variables for different levels of slagging, any ETC value can be used. The uniform ash deposit layer has only theoretical significance. For the non-uniform ash deposit, the results of numerical simulation are similar for the same ratio $q_{w,m}/q_{w,m0}$ and if the ratio of the thicknesses for every pair of the surface zones is constant. These conditions also show when the results of numerical simulations do not depend on the ETC value (or coefficient $a_{0,i}$). When the objective of the investigation is to find the heat exchange for a particular boiler, the exact ETC value is important.

The influence of the shape of the functional dependence of ETC on temperature was not investigated. It is believed that the conclusions would be the same for any other shape of the ETC curve.

4. Conclusions

The combined influence of the deposit thickness and the ETC on temperature was examined in the paper. Three curves were formed on the basis of the available data in literature. The distribution of the ash deposit thicknesses were formed from the adopted base normal distribution, $N(1.0;0.3)$. For every type of the ETC curve, three distributions of the deposit thicknesses were formed. For all distributions formed, the variation coefficient was kept constant.

For the same mean wall flux, the means of the flame temperature and means of the temperature at the furnace exit are approximately the same, in accordance with the heat exchange in the furnace. Also, for the same mean wall fluxes, the means of the wall variables are similar. On the other hand, there is a small difference in the distribution of the wall variables when different ETC values are used. The maximal mean relative difference was obtained for the wall fluxes and it was less than 2%.

The investigation shows that the level of slagging could be defined by the ratio $q_{w,m}/q_{w,m0}$, where $q_{w,m0}$ (kW m^{-2}) is the mean wall flux for the clean wall. For the uniform thickness of the ash deposit, the results of numerical simulations are similar for the same ratio $q_{w,m}/q_{w,m0}$, regardless of the ETC values (or coefficient $a_{0,i}$). For the non-uniform thicknesses, the results of numerical simulations are similar for the same ratio $q_{w,m}/q_{w,m0}$ and for the same ratio of the thicknesses of the corresponding pairs of the surface zones. These conditions show when the results of the numerical simulation do not depend on the ETC values.

When the objective of the investigation is to find the variables for different levels of slagging, any ETC value can be used. The accurate ETC values are important when the goal of the investigations is to find the radiative heat exchange for a particular boiler. For example, if it is found that the thickness of the uniform (or non-uniform equivalent) ash deposit is around 5 mm, then curve A cannot be used.

In the future work, efforts will be made to determine the ETC values by calculation, taking into consideration the particle size smaller than those used in experimental investigations.

Acknowledgements

The research was funded by the Ministry of Science, Technological Development and Innovation of the Republic of Serbia (Contract Annex: 451-03-136/2025-03/200017).

Nomenclature

a	coefficient
k	turbulent kinetic energy [m^2 s^{-2}]
K_{ef}	effective thermal conductivity (W m^{-1} K^{-1})
l_d	deposit thickness (mm)
N	number
$N(;)$	normal distribution
q	flux (W m^{-2})
T	temperature (K)

Greek symbols

ϵ	emissivity (-)
ε	turbulent energy dissipation rate [m^2 s^{-3}]
η	variable
μ	mean (mm)
σ	standard deviation (mm)
δ	difference (%)

Subscripts

b	base
cv	control volume
cr	curve
f	furnace
fe	furnace exit plane
m	mean
mf	mean flux
m,0	mean for clean wall
sw	solid wall
w	wall

Abbreviations

ETC	effective thermal conductivity

References

[1] Raask, E., Minerals Impurities in Coal Combustion, Hemisphere Publishing Corporation, New York, 1985

[2] Sarofim, A. F., Helble, J. J., Mechanisms of Ash and Deposition Formation, *Proceedings, Engineering Foundation Conference*, Solihull, England, June 20th-25th, 1993, pp. 567-582

[3] Prasolov, R. S., Vainshenker, I. A., The Thermal Conductivities and Fractional Composition of Ash Deposits on Pipes and of Laboratory Ashes from Certain Fuels, *Teploenergetika*, 7 (1960), 3, pp. 80-83

[4] Golovin, V. N., Investigation of Tube Fouling in a TP-90 Boiler, *Teploenergetika*, 11 (1964), 3, pp. 23-28

[5] Abryutin, A. A., Karasina, E. S., Thermal Conductivity and Thermal Resistance of Ash Deposits in Boiler Furnaces, *Teploenergetika*, 17 (1970), 12, pp. 36-39

[6] Boow, J., Goard, P. R. C., Fireside Deposits and Their Effect on Heat Transfer in a Pulverized-Fuel-Fired Boiler. Part III: The Influence of the Physical Characteristics of the Deposit on Its Radiant Emittance and Effective Thermal Conductance, *Journal of the Institute of Fuel*, 42 (1969), 346, pp. 412-419

[7] Anderson, D. W., et al., Effective Thermal Conductivity of Cal Ash Deposits at Moderate to High Temperatures, *Journal of Engineering for Gas Turbines and Power*, 109 (1987), 2, pp. 215-221

[8] Rezaei, H. R., et al., Thermal Conductivity of Coal Ash and Slugs and Models Used, *Fuel*, 79 (2000), 13, pp. 1697-1710

[9] Cundick, D. P., et al., Thermal Transport to a Reactor Wall with a Time Varying Ash Layer, *Proceedings, 5th US Combustion Meeting*, San Diego, California, USA, March 25 th-28th, 2007, pp. 3353-3368

[10] Robinson, A. L., et al., In situ Measurements of the Thermal Conductivity of Ash Deposits Formed in a Pilot-Scale Combustor, in Impact of Mineral Impurities in Solid Fuel Combustion, eds. Gupta, R.S., Wall, T. F., Baxter, L., Kluwer Academic/Plenum Publishers, New York, 1999, pp. 485-496

[11] Robinson, A. L., et al., Experimental Measurements of the Thermal Conductivity of Ash Deposits: Part 2. Effects of Sintering and Deposit Microstructure, *Energy & Fuels*, 15 (2001), 1, pp. 75-84

[12] Robinson, A. L., et al., Experimental Measurements of the Thermal Conductivity of Ash Deposits: Part 1. Measurement Technique, *Energy & Fuels*, 15 (2001), 1, pp. 66-74

[13] Robinson, A. L., et al., In Situ Measurements of the Thermal Conductivity of Ash Deposits, Twenty-Seventh Symposium (International) on Combustion, 27 (1998), 2, pp. 1727-1735

[14] Richards, G. H., et al., Simulation of Ash Deposit Growth in a Pulverized Coal-Fired Pilot Scale Reactor, *Energy & Fuels*, 7 (1993), 6, pp. 774-781

[15] Ots, A., Thermophysical Properties of Ash Deposit on Boiler Heat Exchange Surfaces, *Proceedings, International Conference on Heat Exchanger Fouling and Cleaning*, Crete Island, Greece, June 5th -10th, 2011, pp. 150-155

[17] Furmanski, P., Thermal and Radiative Properties of Ash Deposits on Heat Transfer Surfaces of Boilers, *Journal of Power Technologies*, 79 (1995), pp. 1-27

[16] Kaye, G. W. C., Laby, T. H., Tables of Physical and Chemical Constants, Longman, London, 1995

[18] Afifi, M. D., et al., The Effects of Thermal Radiation, Thermal Conductivity, and Variable Viscosity in Ferrofluid in Porous Medium under Magnetic Field, *World Journal of Engineering*, 22 (2023), 1, pp. 218-231

[19] Jalili, B., et al., An Investigation into a Semi-Porous Chanell's Forced Convection of Nano Fluid in the Presence of a Magnetic Field as a Result of Heat Generation, *Scientific Reports*, 13 (2023), 18505

[20] Incropera, F. P., et al., Fundamentals of Heat and Mass Transfer, sixth ed., John Wiley &Sons, New York, 2007

[21] Touloukian, Y. S., Powell, R. W., Ho, C. Y., Klemens, P. G., Thermophysical Properties of Matter, Volume 2, IFI/Plenum Publishing Corporation, New York, 1970

[22] Crnomarkovic, N. Dj, et al., Influence of the Temperature Fluctuations on the Flame Temperature and Radiative Heat Exchange inside a Pulverized Coal-Fired Furnace, *Thermal Science*, 27 (2023), 6A, pp. 4539-4549

[23] Crnomarkovic, N., et al., New Application Method of the Zonal Model for Simulations of Pulverized Coal-Fired Furnaces Based on Correction of Total Exchange Areas, *International Journal of Heat and Mass Transfer*, 149, 119192, 2020

[24] Crnomarković, N. Đ., et al., Numerical Determination of the Impact of the Ash Deposit on the Furnace Walls to the Radiative Heat Exchange inside the Pulverized Coal Fired Furnace, *Proceedings, International Conference Power Plants 2014*, Zlatibor, Serbia, October 28th-31st, 2014, pp. 1-12

[25] Crnomarković, N. Đ., et al., Influence of the Ash Deposit Type on the Numerical Simulation Results of a Pulverized Coal-Fired Furnace, *Proceedings, International Conference Power Plants 2021*, Belgrade, Serbia, November 17th - 18th 2021, pp. 365-376

[26] Press, W. H., et al., Numerical Recipes, The Art of Scientific Computing, Cambridge, New York, 1986

[27] Crnomarkovic, N. Dj., et al., Determination of the Sootblower Activation Moment for Biomass Co-Firing in a Pulverized Coal Furnace, *Thermal Science*, 27 (2023), 1B, pp. 755-766

Paper submitted: 26.12.2024
Paper revised: 12.03.2025
Paper accepted: 18.03.2025